PySHS : A Python Open Source Software For Second Harmonic Scattering

*Lotfi Boudjema, Hanna Aarrass, Marwa Assaf, Marie Morille, Gaelle Martin-Gassin, Pierre-Marie Gassin**

ICGM, ENSCM, CNRS, Univ. Montpellier, Montpellier, France

AUTHOR INFORMATION

Corresponding Author:

*pierre-marie.gassin@enscm.fr

ABSTRACT: PySHS package is a new python open source software which simulates the Second Harmonic Scattering (SHS) of different kind of colloidal nano-object in various experimental configuration. This package is able to compute polarization resolved at a fixed scattered angle or angular distribution for different polarization configurations. This article presents the model implemented in the PySHS software, and gives some computational examples. A comparison between computational results and experimental data concerning molecular dye intercalated inside liposomes membrane is presented to illustrate the possibilities that are given by pySHS.

1 Introduction

Nonlinear light scattering methods and in particular Second Harmonic Scattering (SHS) has been widely used to investigate solvation[1], hydration[2] and correlation[3-7] of molecule in solution[8], self assembly[9-10], interfacial properties of small particles[11-14] , droplets in liquids[15-16] , biological membranes[17-21] or structuration of materials[22-24]. Numerous models[25-30] have been developed to interpret experimental data and in particular angular distribution and polarization dependence of the second harmonic scattered light. The understanding of such variation allows the recovery of important properties about the symmetry[31], the organization[9] and/or the correlation[5-7] of the nano-objects probed. Some of these models have also been implemented in software to compute the SHS intensity, in particular in the NLS_simulate software[32-33] or HRS_Computing software[34]. The NLS_simulate software computes the SHS angular dependence for a sphere using the Nonlinear Rayleigh Gans Debye approximation[33, 35]. In the HRS_computing software, the program computes the polarization resolved SHS intensity for any supramolecular structure build as a sum of correlated individual molecules under the assumption that the correlation length is small in regards to the incident wavelength. In this article, a new free python based program named PySHS[36] is presented. It is able to compute the two kind of calculation discussed above and to go further in the computational possibility because no assumption about the size of the nano-object is done. Indeed, PySHS has been developed in order to compute SHS of different class of nano-objects: uncorrelated molecules in solution in the *HRS module*, supramolecular assemblies in the *SHS module*, Second Harmonic Light scattered by the surface of colloidal spheres in the *SPHERE module*. All the calculations can be done in different experimental configurations: polarization resolved at a fixed scattered angle or angular distribution for different polarization configurations. This article presents the equation implemented in the PySHS software, and gives some

computational examples useful to interpret experimental data concerning the assembly of molecular dye intercalated inside liposomes.

2) The PySHS program

2.1) General notation and configuration

This first part will review the different calculation implemented in the SHS module and sphere module of the PySHS package and the notation used are described in Figure 1.

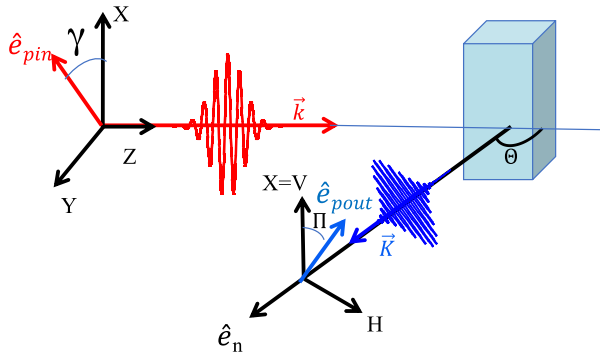

Figure 1. The notation used in the laboratory frame

The fundamental light at the ω frequency is defined by its wave vector $\vec{k} = k\hat{e}_z$ and its polarization direction $\hat{e}_{pin}$. The input polarization angle γ is equal to the angle between $(\hat{e}_X, \hat{e}_{pin})$. The second harmonic scattered light at the 2ω frequency is defined by its wave vector $\vec{K} = K\hat{e}_n$ and the angle $(\hat{e}_z, \hat{e}_n)$ defines the scattered angle Θ. The polarization of the second harmonic scattered light is defined by $\hat{e}_{pout}$ and the output polarization angle Π is equal to the angle between $(\hat{e}_X, \hat{e}_{pout})$. For simplicity, we referred $\Pi = 0°$ as V_{out} polarization state and $\Pi = 90°$ as H_{out} polarization state. In the laboratory frame, we have the following relation:

$$\hat{e}_n = \begin{pmatrix} 0 \\ \sin(\Theta) \\ \cos(\Theta) \end{pmatrix} \qquad \hat{e}_{pin} = \begin{pmatrix} \cos(\gamma) \\ \sin(\gamma) \\ 0 \end{pmatrix} \qquad \hat{e}_{pout} = \begin{pmatrix} \cos(\Pi) \\ \sin(\Pi)\cos(\Theta) \\ \sin(\Pi)\sin(\Theta) \end{pmatrix} \qquad \text{(1-a,b,c)}$$

The scattered wave vector $\overrightarrow{\Delta k}$ is defined as follow:

$$\overrightarrow{\Delta k} = 2\vec{k} - \vec{K} = \begin{pmatrix} 0 \\ -K\sin(\Theta) \\ 2\mathrm{k} - \mathrm{K}\cos(\Theta) \end{pmatrix} \qquad (2)$$

2.2) Calculation for N fully correlated molecules in a supramolecular assembly: *SHS module*

The Second Harmonic Scattering of N fully correlated molecules in solution can be expressed as

$$I_{SHS}(\hat{e}_{pin}, \hat{e}_{pout}, \hat{e}_n) = I_{SHS}(\gamma, \Pi, \Theta) = \langle \vec{\beta}_{eff}(\gamma, \Pi, \Theta).\vec{\beta}^*_{eff}(\gamma, \Pi, \Theta) \rangle \qquad (3)$$

with the $\vec{\beta}_{eff}$ vector defined as:

$$\vec{\beta}_{eff}(\gamma, \Pi, \Theta) = (\hat{e}_n \times \overleftrightarrow{\beta_t}_{Labo} : \hat{e}_{pin}\hat{e}_{pin} \times \hat{e}_n) \qquad (4)$$

This $\vec{\beta}_{eff}$ vector is determined by the total hyperpolarizability tensor of the N molecules assembly $\overleftrightarrow{\beta_t}_{Labo}$ expressed in the laboratory frame which can be itself be expressed in a mesocopic frame $\overleftrightarrow{\beta_t}_{meso}$ as depicted in Figure 3.

$$\overleftrightarrow{\beta_t}_{meso} = \sum_j^N \overleftrightarrow{\beta_j} e^{i\overrightarrow{\Delta k}.\overrightarrow{r'}_j} \qquad (5)$$

Here $\overleftrightarrow{\beta_j}$ is the second order hyperpolarisability of the molecule j located at the position $\overrightarrow{r'}_j$ expressed in the mesoscopic frame.

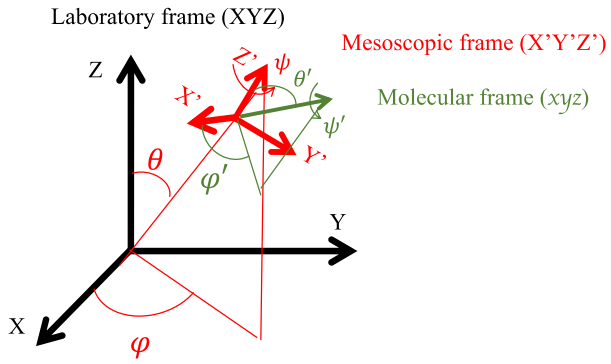

Figure 3. Definition of the angles ($\varphi \quad, \theta \quad, \psi \quad$) and ($\varphi'_j, \theta'_j, \psi'_j$)which describe the orientation of the scattered object in the different frames.

The hyperpolarisability tensor components in the different frames are linked according:

$$\beta_{IJK,meso}(\varphi', \theta', \psi') = \sum_i \sum_j \sum_k T(\varphi', \theta', \psi') T(\varphi', \theta', \psi') T(\varphi', \theta', \psi') \beta_{ijk,micro} \quad (6)$$

$$\beta_{IJK,Labo}(\varphi, \theta, \psi) = \sum_i \sum_j \sum_k T(\varphi, \theta, \psi) T(\varphi, \theta, \psi) T(\varphi, \theta, \psi) \beta_{ijk,meso} \quad (7)$$

The transformation matrix $T(\varphi, \theta, \psi)$ is:

$$T(\varphi, \theta, \psi) =$$

$$\begin{pmatrix} \cos(\psi)\sin(\varphi) - \cos(\theta)\cos(\varphi)\sin(\psi) & \cos(\theta)\cos(\psi)\cos(\varphi) + \sin(\varphi)\sin(\psi) & \sin(\theta)\sin(\varphi) \\ -\cos(\varphi)\cos(\psi) - \cos(\theta)\sin(\varphi)\sin(\psi) & \cos(\theta)\cos(\psi)\cos(\varphi) - \cos(\varphi)\sin(\psi) & \sin(\theta)\sin(\varphi) \\ \sin(\theta)\sin(\psi) & -\sin(\theta)\cos(\psi) & \cos(\theta) \end{pmatrix}$$

(8)

Finally, the bracket in formula (3) means the average over all the orientation of the scattered molecule.

$$\langle . \rangle = \int_{\theta=0}^{\pi} \int_{\varphi=0}^{2\pi} \int_{\psi=0}^{2\pi} . \sin\theta d\theta d\varphi d\psi \quad (9)$$

To perform the I_{SHS} calculation, the user needs to specify the position $\vec{r'}_j = (x'_j, y'_j, z'_j)$ and orientation ($\varphi'_j, \theta'_j, \psi'_j$) of each molecule in the mesoscopic frame. Two ways are implemented to perform the $I_{SHS}(\gamma, \Pi, \Theta)$ calculation: the first way implemented in the SHS program of PySHS

package explicitly computes I_{SHS} according to equations (3-9). The second way implemented in the SHSlinear program, uses the approach detailed in these references[6, 23, 31] and in the HRS_Computing software[34], approximates the exponential term in equation (5) by:

$$e^{i\overrightarrow{\Delta k}.\vec{r}_j} \cong 1 + \overrightarrow{\Delta k}.\overrightarrow{r'}_j + \cdots \quad (10)$$

This last calculation is only valid in the domain where $\overrightarrow{\Delta k}.\overrightarrow{r'}_j$ is small compared to 1, *ie* if the characteristic size of the molecular assembly is small compared to the incident wavelength. Taking the molecular hyperpolarizability, the position and orientation of each molecule in the supramolecular assembly as input parameters, the SHS and SHSlinear programs can compute the polarization resolved plot or the scattered angle plot. For the polarization plot, the outputs of the program are the coefficients $a_\Pi^\Theta, b_\Pi^\Theta, c_\Pi^\Theta$ and $I_2^{\Theta,\Pi}$, $I_4^{\Theta,\Pi}$defined in this work[31]. Indeed, the SHS intensity exhibits the equivalent following dependencies with the input polarization angle γ :

$$I_{SHS}\ \ (\gamma, \Pi, \Theta) = a_\Pi^\Theta.cos^4(\gamma) + b_\Pi^\Theta.cos^2(\gamma)sin^2(\gamma) + c_\Pi^\Theta.sin^4(\gamma) \quad (11)$$

$$I_{SHS}\ \ (\gamma, \Pi, \Theta) = i_0^{\Theta,\Pi}\left(1 + I_2^{\Theta,\Pi}\cos(2\gamma) + I_4^{\Theta,\Pi}\cos(4\gamma)\right) \quad (12)$$

The link between these two descriptions are given by:

$$i_0^{\Theta,\Pi} = \frac{1}{8}\left(3a_\Pi^\Theta + b_\Pi^\Theta + 3c_\Pi^\Theta\right) \quad (13)$$

$$I_2^{\Theta,\Pi} = \frac{4(a_\Pi^\Theta - c_\Pi^\Theta)}{(3a_\Pi^\Theta + b_\Pi^\Theta + 3c_\Pi^\Theta)} \quad (14)$$

$$I_4^{\Theta,\Pi} = \frac{(a_\Pi^\Theta - b_\Pi^\Theta + c_\Pi^\Theta)}{(3a_\Pi^\Theta + b_\Pi^\Theta + 3c_\Pi^\Theta)} \quad (15)$$

The full expression of the $a_\Pi^\Theta, b_\Pi^\Theta, c_\Pi^\Theta$ coefficients are given in SI. For an angular dependency study, the output of the program is the dependency $I_{SHS}\ \ (\Theta)$ for different combination of polarization state (γ, Π): $(0°, 0°)$; $(90°, 0°)$; $(0°, 90°)$; $(90°, 90°)$.

2.3) Calculation for the surface of colloidal sphere in solution: *SPHERE module*

PySHS package offers the possibility to compute the SHS intensity of homogeneous spheres in solution. To perform this calculation, an effective nonlinear susceptibility $\overleftrightarrow{\Gamma^{(2)}}$ is introduced as proposed in this work[25], it represents the nonlinear response of the entire sphere surface:

$$\overleftrightarrow{\Gamma^{(2)}} = \oiint_{surface\ of\ the\ sphere} \overleftrightarrow{\chi^{(2)}} . e^{i\overrightarrow{\Delta k}.\vec{r}} d\vec{r} \quad (16)$$

where $\overleftrightarrow{\chi^{(2)}}$ is the surface second order nonlinear susceptibility of the sphere. Using the same formalism as above, The SHS intensity is expressed with the same equation (3) where $\vec{\beta}_{eff}$ is now expressed as:

$$\vec{\beta}_{eff} = (\hat{e}_n \times \overleftrightarrow{\Gamma^{(2)}} : \hat{e}_p \hat{e}_p \times \hat{e}_n) \quad (17)$$

The *SPHERE* program in the PySHS package takes the surface second order nonlinear susceptibility and the radius of the sphere as input parameters and computes the same quantities as define above in equations (11-14)

3) Results and discussion section

Some results illustrating the possibilities given by the PySHS package are presented and confronted with experimental data. This part focuses on the SHS polarization plot in the right angle direction for spherical supramolecular assemblies in order to interpret experimental results concerning the organization of molecular dyes inclusion into the membrane of liposomes. The Figure 4 shows the polarization plot computed with the programs implemented in PySHS package for a 50 nm radius sphere. An input file containing the position and orientation of 100 molecules

equally spaced onto the sphere surface and radially oriented was generated by the script provided in the package. The other input parameters of the calculations are the refractive index set to 1.33, the incident wavelength set to 800 nm and the hyperpolarizability of the molecule which is assumed to have only the β_{ZZZ} component to be no zero.

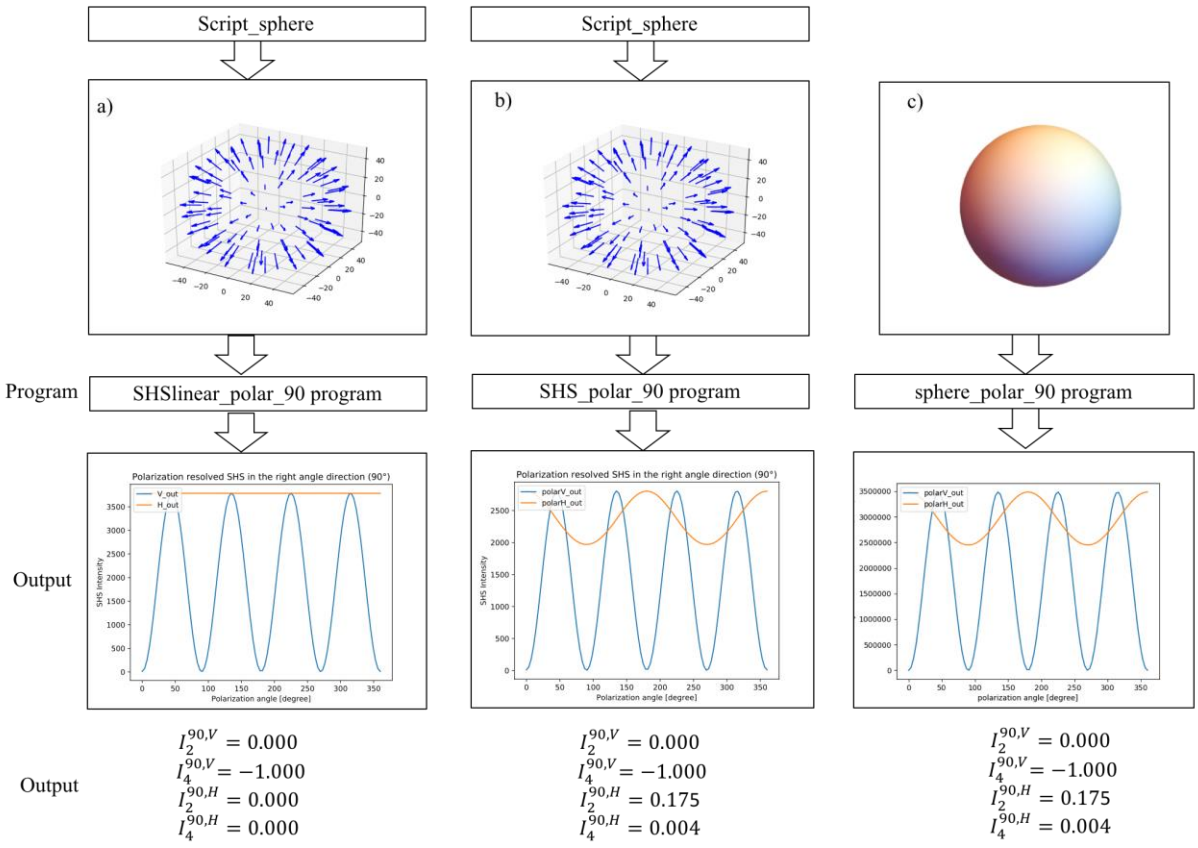

Figure 4. Computational polarization plot obtained with 3 different calculations: a) SHSlinear program equation (3-9) with the equation 10 approximation, b) SHS program equation (3-9) with no approximation and c) sphere program equation (15-16). The input parameters are: scattered angle=90°, radius=50 nm, refractive index n=1.33, Incident wavelength=800 nm, and hyperpolarizability tensor, β_{zzz}=1 all the other component equal to 0.

The comparison between simulations a) and b) shows that the polarization plot change for the Hout polarization state in particular because the $I_2^{90,\mathrm{H}}$ coefficient is no null for the b) simulation.

This result shows that the deviation induced by the approximation of equation (10) is not negligible and the program SHSlinear is thus not really valid for a 50 nm radius sphere. The results given by the HRS_Computing software are the same as the SHSlinear program of the PySHS package which is expected as the equations implemented are the same. This point is developed in the SI where both HRS_Computing software and NLS_Simulate software are compared with the PySHS calculation. Nevertheless, for the study of only Vout polarization state, the SHSlinear program gives the same results as the complete model. In the following, all the computations are done with the complete model, ie with the SHS program. The simulations b) and c) give exactly the same results at the 3rd digit after the decimal point although the two approaches are not the same. It just shows that 100 dipoles equally spaced onto a sphere is equivalent to an homogenous sphere. We have also tested the case of few dipoles spaced onto a sphere, and we found the same results as given in this previous work[31] concerning the evolution of I_2 and I_4 parameters with the number of dipoles onto the sphere. When this number N is superior to 10, these quantities reach the asymptote of the homogeneous sphere given by the sphere program. To quantify the effect of the order/disorder of the assembly onto the sphere, a script provided in the PySHS package generates randomly the position and orientation of the molecules with a normal distribution around the radial direction. This distribution is characterized by its standard deviation σ. Figure 5 presents the polarization plot generated with the SHS program for different disorder of the assembly described by σ.

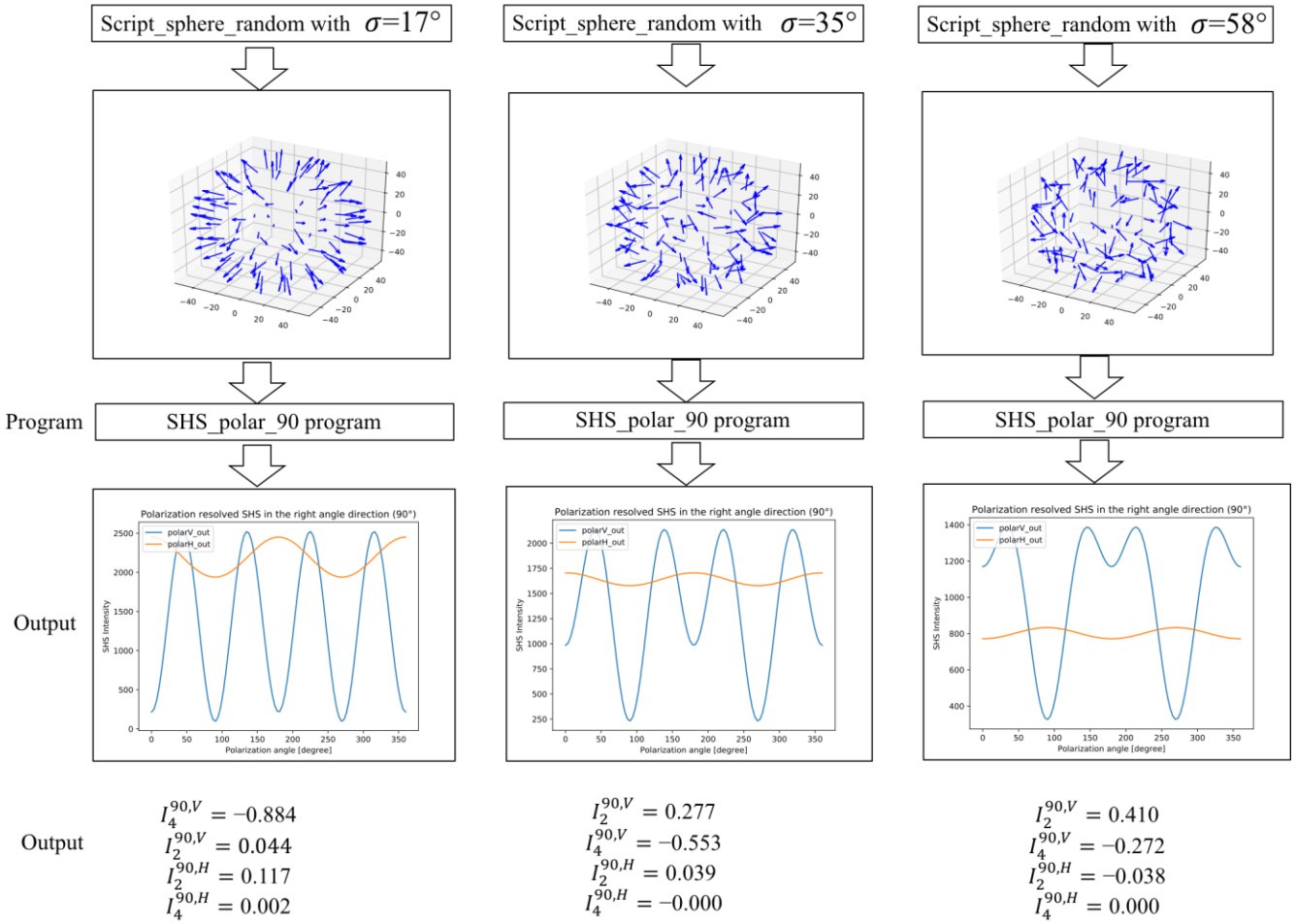

Figure 5. Computational polarization plot obtained with different molecular assembly disorders: a) σ=17°, b) σ=35° and c) σ=58°. The other input parameters are the same as in Figure 4.

The polarization plots evolve with the disorder of the assembly in the following direction: $I_2^{90,\mathrm{V}}$ increases whereas $I_2^{90,\mathrm{H}}$and $I_4^{90,\mathrm{V}}$ decreases. At a totally disorder organization, this evolution approaches the case of fully uncorrelated molecule which gives in the case of only no zero β_{zzz}: $I_2^{90,\mathrm{V}} = 2/3$ and $I_4^{90,\mathrm{V}}$=$I_2^{90,\mathrm{H}}$=$I_4^{90,\mathrm{H}} = 0$. Introducing the disorder of the molecular organization onto the sphere is not enough to explained the experimental data presented below. So, a study about the variation of the ideal spherical arrangement is discussed in Figure 6. To do that, the

global arrangement is changed from spherical geometry to spheroid geometry characterized with its two radius a and c. In this study, the dipoles are radially oriented as in Figure 4 simulations.

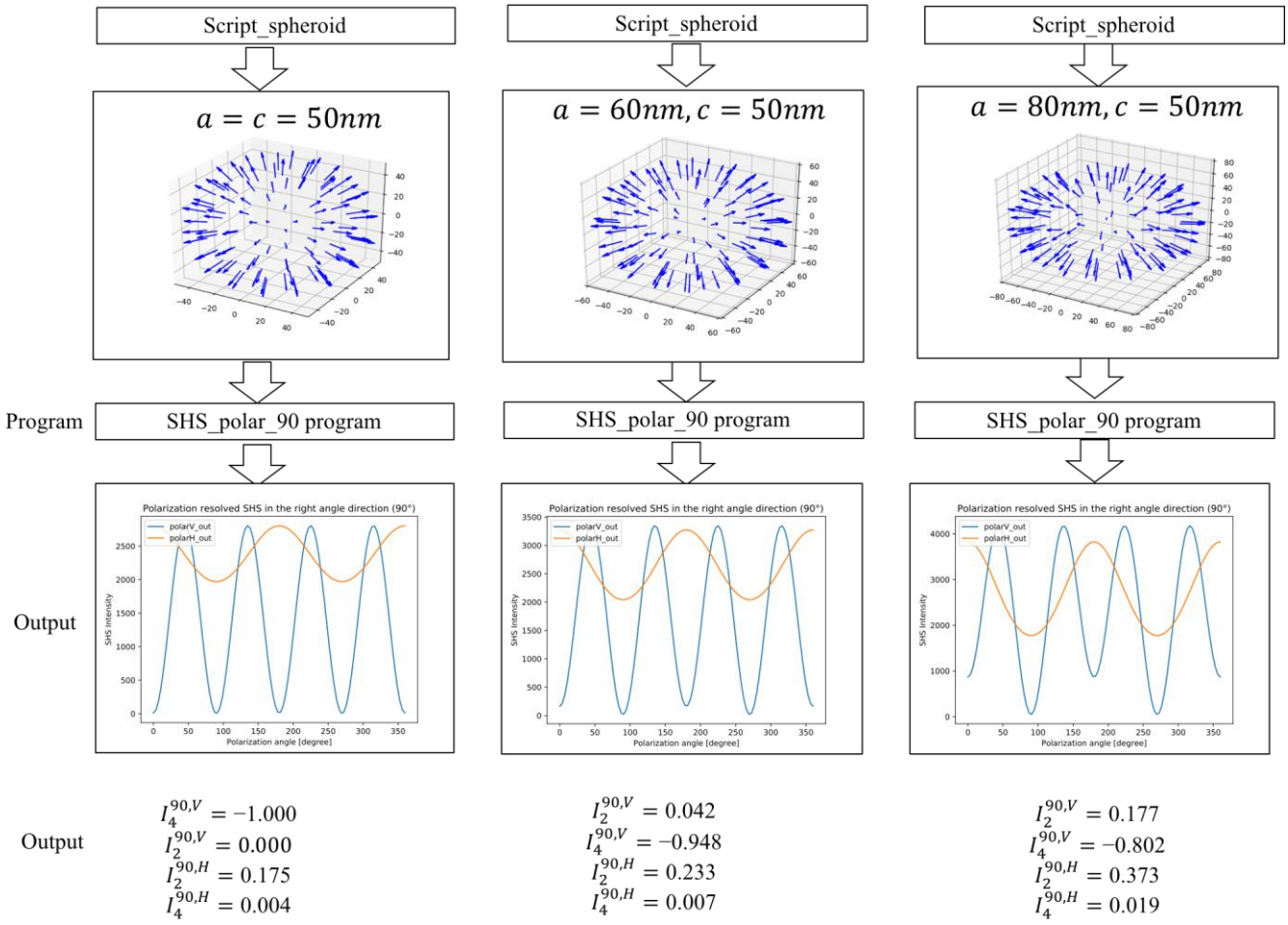

Figure 6. Computational polarization plot obtained with different molecular assemblies: a) spherical assembly, b) spheroid assembly with radius equal to 60 and 50 nm. c) spheroid assembly with radius equal to 80 and 50 nm. The other input parameters are the same as in Figure 4 and 5.

Increasing the difference of the pure spherical geometry induces the following evolution: $I_2^{90,V}$ $I_2^{90,H}$ and $I_4^{90,H}$ increase whereas $I_4^{90,V}$ decreases. When these two elements, disorder and deviation to no spherical geometry are taken into account, the experimental data, *ie* both the Hout and Vout

polar plot, presented in Figure 7 can be satisfactory interpreted with the computational model. Figure 7 presents experimental data concerning dye organization onto liposome membrane. The molecular dye, presented in Figure 7a), is the trans-4-[4-(Dibutylamino)styryl]-1-methylpyridinium iodide simply referred as DIA-4 in the following. This dye has been brought together with a solution of 55 +/- 5 nm radius DOPG liposomes in PBS buffer and the SHS polarization plots are presented in Figure 7c. All the experimental details concerning the sample preparation are given in SI. The SHS experimental setup has been described elsewhere[2, 37], and the experimental data has been treated as follow: the incoherent contribution of the liposomes solution, i.e. the HRS contribution has been removed, so that the experimental point can be directly compared with the computational model. The best fit is obtained for a spheroid arrangement characterized with radius a=70 nm and c=50 nm and with a disorder characterized by standard deviation σ=12°.

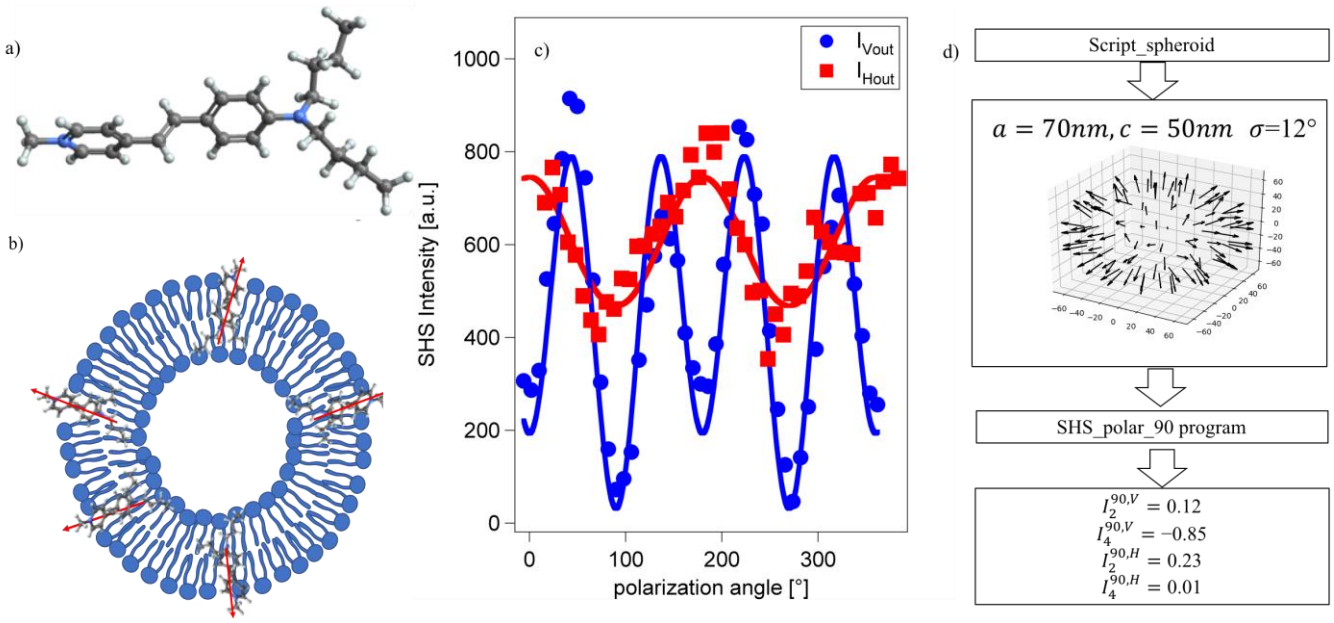

Figure 7. a) The DIA-4 molecule. b) A schematic representation of the system studied with polarization resolved SHS. c) Experimental polarization resolved SHS for a solution of 5 □M of

DIA-4 with 5.10^{10} DOPG 50 nm radius liposomes in PBS buffer. The circular and rectangular markers are the experimental data and the lines are the polarization plot simulated with PySHS package d) Simulation scheme that reproduced the experimental data: a spheroid arrangement with a disorder index σ=12°.

Conclusion

This article presents the numerical PySHS package which has been developed in order to compute SHS intensity dependence with polarization state and angular scattering. The specificity of this new package has been discussed and compared with other available software. This new code, freely accessible on internet, allows more accurate computation especially in the case of large supramolecular structure for which no size limitation is required. It gives also more possibility of configuration to be simulated (in the right angle or in forward direction) and different scripts provided in the package can simulate various geometry. To demonstrate the usefulness of its package, the polarization plot for different supramolecular organizations onto a sphere or spheroid object are presented in this publication. Especially, the numerical results are compared with experimental results concerning dye inclusion inside liposome bilayer. This comparison shows that both the disorder parameter and the deviation from the spherical geometry have to be taken into account to explain the experimental data. We hope that this work will stimulate the SHS community, will encourage the reader to try PySHS package, and help the experimenter to interpret their SHS results.

ASSOCIATED CONTENT

Funding Sources

Financial support for this work by the ANR project **CAMOMILS (ANR-15-CE21-0002)** is greatly acknowledged.

ACKNOWLEDGMENT

We warmly thank Pierre-Francois Brevet for fruitful regular discussions about simulation and nonlinear optics.

ABBREVIATIONS

SHS, second harmonic scattering; HRS, hyper Rayleigh scattering; PBS, phosphate buffered saline; DOPG, 1,2-Dioleoyl-sn-glycero-3-phospho-rac-(1-glycerol) sodium salt

REFERENCES

1. Borgis, D.; Belloni, L.; Levesque, M., What Does Second-Harmonic Scattering Measure in Diluted Electrolytes? *The Journal of Physical Chemistry Letters* **2018**, *9*, 3698-3702.
2. Gassin, P.-M.; Prelot, B.; Gregoire, B.; Martin-Gassin, G., Second-Harmonic Scattering Can Probe Hydration and Specific Ion Effects in Clay Particles. *The Journal of Physical Chemistry C* **2020**, *124*, 4109-4113.
3. Shelton, D. P., Hyper-Rayleigh Scattering from Correlated Molecules. *The Journal of Chemical Physics* **2013**, *138*, 154502.
4. Shelton, D. P., Long-Range Orientation Correlation in Water. *The Journal of Chemical Physics* **2014**, *141*, 224506.
5. Tocci, G.; Liang, C.; Wilkins, D. M.; Roke, S.; Ceriotti, M., Second-Harmonic Scattering as a Probe of Structural Correlations in Liquids. *The Journal of Physical Chemistry Letters* **2016**, *7*, 4311-4316.
6. Duboisset, J.; Brevet, P.-F., Salt-Induced Long-to-Short Range Orientational Transition in Water. *Physical Review Letters* **2018**, *120*, 263001.
7. Chen, Y., et al., Electrolytes Induce Long-Range Orientational Order and Free Energy Changes in the H-Bond Network of Bulk Water. *Science Advances* **2016**, *2*, e1501891.
8. Clays, K.; Persoons, A., Hyper-Rayleigh Scattering in Solution. *Physical Review Letters* **1991**, *66*, 2980-2983.
9. Moris, M.; Van Den Eede, M.-P.; Koeckelberghs, G.; Deschaume, O.; Bartic, C.; Van Cleuvenbergen, S.; Clays, K.; Verbiest, T., Harmonic Light Scattering Study Reveals Structured Clusters Upon the Supramolecular Aggregation of Regioregular Poly(3-Alkylthiophene). *Communications Chemistry* **2019**, *2*, 130.
10. Revillod, G.; Duboisset, J.; Russier-Antoine, I.; Benichou, E.; Bachelier, G.; Jonin, C.; Brevet, P.-F., Multipolar Contributions to the Second Harmonic Response from Mixed Dia−Sds Molecular Aggregates. *The Journal of Physical Chemistry C* **2008**, *112*, 2716-2723.
11. Cole, W. T. S.; Wei, H.; Nguyen, S. C.; Harris, C. B.; Miller, D. J.; Saykally, R. J., Dynamics of Micropollutant Adsorption to Polystyrene Surfaces Probed by Angle-Resolved Second Harmonic Scattering. *The Journal of Physical Chemistry C* **2019**, *123*, 14362-14369.

12. Gonella, G.; Dai, H.-L., Second Harmonic Light Scattering from the Surface of Colloidal Objects: Theory and Applications. *Langmuir* **2014**, *30*, 2588-2599.
13. Eisenthal, K. B., Second Harmonic Spectroscopy of Aqueous Nano- and Microparticle Interfaces. *Chemical Reviews* **2006**, *106*, 1462-1477.
14. Marchioro, A.; Bischoff, M.; Lütgebaucks, C.; Biriukov, D.; Předota, M.; Roke, S., Surface Characterization of Colloidal Silica Nanoparticles by Second Harmonic Scattering: Quantifying the Surface Potential and Interfacial Water Order. *The Journal of Physical Chemistry C* **2019**, *123*, 20393-20404.
15. Roke, S.; Gonella, G., Nonlinear Light Scattering and Spectroscopy of Particles and Droplets in Liquids. *Annual Review of Physical Chemistry* **2012**, *63*, 353-378.
16. Zdrali, E.; Etienne, G.; Smolentsev, N.; Amstad, E.; Roke, S., The Interfacial Structure of Nano- and Micron-Sized Oil and Water Droplets Stabilized with Sds and Span80. *The Journal of Chemical Physics* **2019**, *150*, 204704.
17. Wilhelm, M. J.; Gh., M. S.; Dai, H.-L., Influence of Molecular Structure on Passive Membrane Transport: A Case Study by Second Harmonic Light Scattering. *The Journal of Chemical Physics* **2019**, *150*, 104705.
18. Hamal, P.; Nguyenhuu, H.; Subasinghege Don, V.; Kumal, R. R.; Kumar, R.; McCarley, R. L.; Haber, L. H., Molecular Adsorption and Transport at Liposome Surfaces Studied by Molecular Dynamics Simulations and Second Harmonic Generation Spectroscopy. *The Journal of Physical Chemistry B* **2019**, *123*, 7722-7730.
19. Tarun, O. B.; Okur, H. I.; Rangamani, P.; Roke, S., Transient Domains of Ordered Water Induced by Divalent Ions Lead to Lipid Membrane Curvature Fluctuations. *Communications Chemistry* **2020**, *3*, 17.
20. Okur, H. I.; Tarun, O. B.; Roke, S., Chemistry of Lipid Membranes from Models to Living Systems: A Perspective of Hydration, Surface Potential, Curvature, Confinement and Heterogeneity. *Journal of the American Chemical Society* **2019**, *141*, 12168-12181.
21. Miller, L. N.; Brewer, W. T.; Williams, J. D.; Fozo, E. M.; Calhoun, T. R., Second Harmonic Generation Spectroscopy of Membrane Probe Dynamics in Gram-Positive Bacteria. *Biophysical Journal* **2019**, *117*, 1419-1428.
22. Van Cleuvenbergen, S.; Smith, Z. J.; Deschaume, O.; Bartic, C.; Wachsmann-Hogiu, S.; Verbiest, T.; van der Veen, M. A., Morphology and Structure of Zif-8 During Crystallisation Measured by Dynamic Angle-Resolved Second Harmonic Scattering. *Nat Commun* **2018**, *9*, 3418-3418.
23. Gassin, P.-M.; Prelot, B.; Grégoire, B.; Martin-Gassin, G., Second-Harmonic Scattering in Layered Double Hydroxide Colloids: A Microscopic View of Adsorption and Intercalation. *Langmuir* **2018**, *34*, 12206-12213.
24. de Beer, A. G. F.; de Aguiar, H. B.; Nijsen, J. F. W.; Roke, S., Detection of Buried Microstructures by Nonlinear Light Scattering Spectroscopy. *Physical Review Letters* **2009**, *102*, 095502.
25. Roke, S.; Bonn, M.; Petukhov, A. V., Nonlinear Optical Scattering: The Concept of Effective Susceptibility. *Physical Review B* **2004**, *70*, 115106.
26. Gonella, G.; Dai, H.-L., Determination of Adsorption Geometry on Spherical Particles from Nonlinear Mie Theory Analysis of Surface Second Harmonic Generation. *Physical Review B* **2011**, *84*, 121402.

27. Dadap, J. I.; Shan, J.; Eisenthal, K. B.; Heinz, T. F., Second-Harmonic Rayleigh Scattering from a Sphere of Centrosymmetric Material. *Physical Review Letters* **1999**, *83*, 4045-4048.
28. Dadap, J. I.; Shan, J.; Heinz, T. F., Theory of Optical Second-Harmonic Generation from a Sphere of Centrosymmetric Material: Small-Particle Limit. *J. Opt. Soc. Am. B* **2004**, *21*, 1328-1347.
29. Gonella, G.; Lütgebaucks, C.; de Beer, A. G. F.; Roke, S., Second Harmonic and Sum-Frequency Generation from Aqueous Interfaces Is Modulated by Interference. *The Journal of Physical Chemistry C* **2016**, *120*, 9165-9173.
30. de Beer, A. G. F.; Roke, S., Nonlinear Mie Theory for Second-Harmonic and Sum-Frequency Scattering. *Physical Review B* **2009**, *79*, 155420.
31. Duboisset, J.; Brevet, P.-F., Second-Harmonic Scattering-Defined Topological Classes for Nano-Objects. *The Journal of Physical Chemistry C* **2019**, *123*, 25303-25308.
32. De Beer, A. G. F. R., S. https://www.epfl.ch/labs/lbp/page-89617-en-html/.
33. Beer, A. G. F. d.; Roke, S., Obtaining Molecular Orientation from Second Harmonic and Sum Frequency Scattering Experiments in Water: Angular Distribution and Polarization Dependence. *The Journal of Chemical Physics* **2010**, *132*, 234702.
34. Carrazza, S. D., J. https://en.wikipedia.org/wiki/HRS_Computing.
35. Jen, S. H.; Dai, H.-L.; Gonella, G., The Effect of Particle Size in Second Harmonic Generation from the Surface of Spherical Colloidal Particles. Ii: The Nonlinear Rayleigh-Gans-Debye Model. *The Journal of Physical Chemistry C* **2010**, *114*.
36. Gassin, P. M., Martin-Gassin G. https://www.researchgate.net/profile/Pierre-Marie_Gassin/publication/342742567_PySHS_V11_A_Python_Open_Source_Software_For_Second_Harmonic_Scattering/data/5f046b36a6fdcc4ca453037b/PySHS-V11.zip.
37. Gassin, P.-M.; Bellini, S.; Zajac, J.; Martin-Gassin, G., Adsorbed Dyes onto Nanoparticles: Large Wavelength Dependence in Second Harmonic Scattering. *The Journal of Physical Chemistry C* **2017**, *121*, 14566-14571.

Table of Contents graphic